Biochemical and Biophysical Research Communications 407 (2011) 230–235

Contents lists available at ScienceDirect

Biochemical and Biophysical Research Communications

journal homepage: www.elsevier.com/locate/ybbrc

Probing the structural determinants of yellow fluorescence of a protein from *Phialidium* sp.

Alexey A. Pakhomov *, Vladimir I. Martynov

Chromoproteins Chemistry Research Group, Shemyakin-Ovchinnikov Institute of Bioorganic Chemistry, Russian Academy of Sciences, Moscow, Russia

ARTICLE INFO

Article history:
Received 24 February 2011
Available online 5 March 2011

Keywords:
Fluorescence
Chromophore
Posttranslational modification
Autocatalysis

ABSTRACT

Fluorescent proteins homologous to green fluorescent protein (avGFP) display pronounced spectral variability due to different chromophore structures and variable chromophore interactions with the surrounding amino acids. To gain insight into the structural basis for yellow emission, the 3D structure of phiYFP (λ_{em} = 537 nm), a protein from the sea medusa *Phialidium* sp., was built by a combined homology modeling – mass spectrometry approach. Mass spectrometry of the isolated chromophore-bearing peptide reveals that the chromophore of phiYFP is chemically identical to that of avGFP (λ_{em} = 508 nm). The experimentally acquired chromophore structure was combined with the homology-based model of phiYFP, and the proposed 3D structure was used as a starting point for identification of the structural features responsible for yellow fluorescence. Mutagenesis of residues in the local chromophore environment of phiYFP suggests that multiple factors cooperate to establish the longest-wavelength emission maximum among fluorescent proteins with an unmodified GFP-like chromophore.

1. Introduction

Green fluorescent protein from *Aequorea victoria* (avGFP) and homologous fluorescent proteins (FPs) from Anthozoa have become indispensable tools for live cell imaging [1]. The available emission colors of FPs span most of the visible spectrum, offering a wide array of fluorescent markers [2]. The color variation of FPs is mostly due to different chemical modifications of the chromophore, which is autocatalytically formed from internal amino acids [3]. In avGFP, the chromophore 4-(*p*-hydroxybenzylidene)imidazolinone (*p*-HBI) is generated by cyclization of the polypeptide chain within the Ser-Tyr-Gly sequence [4,5]. GFP-like *p*-HBIs can undergo further posttranslational modifications, as in the case of red-shifted fluorescent proteins [6–10] and chromoproteins [11–15].

Crystallographic and mass spectrometric studies reveal that zFP538, a yellow fluorescent protein from *Zoanthus* sp., contains a three-ring chromophore derived from the DsRed-like chromophore [16]. A conjugation intermediate to that of GFP and DsRed has been proposed to account for the yellow emission of the zFP538 chromophore (λ_{em} = 538 nm). Alternatively, the mutation T203Y (here and hereinafter, the amino acid numbering corresponds to the avGFP sequence), which is located in the vicinity of the avGFP chromophore, may induce a red shift in the emission without covalent modification of *p*-HBI. The emission of the resultant yellow fluorescent protein, YFP, is red-shifted by approximately 20 nm (λ_{em} = 527 nm) relative to avGFP-S65T due to a π-stacking interaction between the chromophore phenolic group and Tyr203 [17]. This observation suggests that, in addition to covalent modifications of the chromophore, chromophore–protein interactions also have a dramatic impact upon FP spectral properties.

Yellow-emitting fluorescent protein phiYFP has recently been cloned from the sea medusa *Phialidium* sp. (class Hydrozoa). It displays an emission maximum at 537 nm [18] – very similar to zFP538 – and can fill in the gap between green- and red-emitting FPs. phiYFP can be particularly useful for live cell multicolor imaging and is suitable as an acceptor in Förster resonance energy transfer (FRET) experiments. High-resolution X-ray crystallographic studies of phiYFP would be beneficial in understanding the structural features that are responsible for the yellow fluorescence. However, in some cases it is extremely difficult to obtain high-quality FP crystals [16], which can subsequently result in poor resolution diffraction data.

To gain insight into the molecular basis for the yellow fluorescence emission of phiYFP, we undertook a study of the protein

Abbreviations: FP, fluorescent protein; avGFP, green fluorescent protein from *Aequorea victoria*; DsRed, red fluorescent protein from *Discosoma* sp.; phiYFP, yellow fluorescent protein from *Phialidium* sp.; *p*-HBI, 4-(*p*-hydroxybenzylidene)imidazolinone; zFP538, yellow fluorescent protein from *Zoanthus* sp.; YFP, yellow fluorescent variant of avGFP; ESPT, excited-state proton transfer; MS, mass spectrometry.

* Corresponding author. Address: Chromoproteins Chemistry Research Group, Shemyakin-Ovchinnikov Institute of Bioorganic Chemistry, Russian Academy of Sciences, Miklukho-Maklaya 16/10, 117997 Moscow, Russia. Fax: +7 495 336 6166.
E-mail address: alpah@mail.ru (A.A. Pakhomov).

0006-291X/$ - see front matter © 2011 Elsevier Inc. All rights reserved.
doi:10.1016/j.bbrc.2011.03.004

3D structure based on a combination of mass spectrometry and homology modeling. High-resolution mass spectrometry of the isolated chromophore-bearing peptide showed that, unlike zFP538, mature phiYFP contains a GFP-like *p*-HBI chromophore. Incorporation of this chromophore into the constructed model of the protein enabled us to propose a complete 3D model of phiYFP. Further structure-based mutagenesis studies revealed structural determinants that presumably operate in a cooperative manner to establish the red-shifted spectra of phiYFP.

2. Materials and methods

2.1. Protein expression, purification, and mutagenesis

A pQE-30 expression system in *Escherichia coli* (JM-109 DE3) was used to express phiYFP with an N-terminal polyhistidine tag. The recombinant protein was further purified from cell lysates by metal-affinity chromatography on a Ni–NTA resin (Qiagen) according to the manufacturer's protocol. Site-directed mutagenesis was performed with the QuikChange Site-Directed Mutagenesis kit (Stratagene). The resulting plasmids were sequenced to verify mutations.

2.2. Spectroscopy

Absorption spectra for phiYFP and variants were collected at 22 °C in 20 mM Tris–HCl and 100 mM NaCl, (pH 8.0) using a Cary 50 Bio UV/vis spectrophotometer (Varian). The fluorescence measurements were carried out using a Varian Cary Eclipse Fluorescence Spectrophotometer. The *p*Ka of the chromophore was calculated by computer-fitting the absorbance of band B at various pHs to the Henderson–Hasselbalch equation [19].

2.3. Pepsinolysis and chromopeptide isolation

Purified His-tagged phiYFP at 4 mg/mL was denatured by addition of a 0.1 M HCl solution to a final pH of 2.3. Pepsin (Sigma) was then added at a 1:30 (w/w) ratio, and digestion was carried out at room temperature for 24 h. Chromopeptide isolation was performed as described previously [19]. Briefly, digests were applied onto a reverse phase HPLC column (Beckman Ultrasphere ODS) equilibrated with 10 mM sodium phosphate buffer pH 4.0 and peptides were eluted by a linear gradient of acetonitrile in the same buffer. The effluent was monitored at 220 nm and 380 nm. Peptide peaks with absorbance at 380 nm were collected and analyzed by mass spectrometry.

2.4. MALDI mass spectrometry

One microliter each of the chromopeptide and the 2,5-dihydroxybenzoic acid (DHB) matrix (Sigma) dissolved in 0.1% trifluoracetic acid: acetonitrile, 7:3 were mixed on a stainless steel target and air-dried at room temperature. MS experiments were carried out in the reflectron mode on an Ultraflex MALDI TOF/TOF mass spectrometer with LIFT capability (Bruker Daltonics) equipped with an N_2-laser. Mass spectra were acquired in a positive ion mode. Tandem mass spectra were acquired with a basic MALDI-TOF/TOF method comprising the following voltage parameters: ion source I – 8 kV, ion source II – 7.2 kV, lens – 3.4 kV, reflector – 27.5 kV, reflector II – 12.8 kV, LIFT1–19 kV, LIFT2–3.3 kV.

2.5. Sequence analysis and homology modeling

Multiple sequence alignment of GFP-like proteins with known crystal structures was performed using the ClustalW method [20] and a phylogenetic tree was built with the program MegAlign from DNASTAR package (Supplementary Fig. S1). GFP from *A. victoria* proved to have the highest sequence identity with phiYFP (51% identity). Therefore, the atomic coordinates of the avGFP crystal structure (PDB ID: 1EMB) were selected as the template. Pairwise sequence alignment and subsequent homology modeling were performed using MODELLER9v7. The chromophore moiety was introduced as a rigid body in the program mode, which enables heteroatom residue incorporation. Model evaluation was carried out using either the MODELLER objective function or the DOPE assessment score in accordance with the MODELLER manual (http://www.salilab.org/modeller/). Finally, model quality was validated using COOT [21]. The atomic coordinates of the phiYFP homology model are available as a PDB-file in the supplementary data.

3. Results and discussion

3.1. Structure of phiYFP chromophore

Denatured phiYFP was extensively digested with pepsin, and the chromophore-bearing peptide was isolated by HPLC. A MALDI mass spectrum of the chromopeptide contains a peak at $m/z = 1036.5$, which corresponds to a monoisotopic mass of 1035.5 Da. A fragment of the published protein sequence, -Val-Thr-Thr-Leu-[Thr-Tyr-Gly]-Ala-Gln-Cys- [18], is consistent with these mass spectral results, taking into account that the 1035.5 Da mass is 20 Da lower than the value calculated for the unmodified peptide (1055.5 Da) with the same sequence. These results suggest that the phiYFP chromophore derives from a post-translational cyclization within the internal tripeptide -[Thr-Tyr-Gly]- followed by dehydration (loss of H_2O, −18 Da) and oxidation (loss of H_2, −2 Da) reactions. The same posttranslational reactions have been reported to take place during biosynthesis of the avGFP chromophore [4,5,20]. Further fragmentation of the 1036.5 m/z parent peak in tandem mass spectrometry produced additional daughter peaks (Supplementary Table S1). These peaks were assigned to "a," "b," "c," and "x," "y" ions. The m/z differences between the neighboring "y" ions are consistent with the consecutive loss of Val, Thr, Thr and Leu. The same comparison of the "a," "b" and "c"-ions revealed the C-terminal sequence of the chromopeptide (Supplementary Table S1). Thus, manual interpretation of the mass differences between adjacent pairs of peaks following MS/MS fragmentation revealed the N-terminal sequence of the chromopeptide to be Val-Thr-Thr-Leu- and the C-terminal sequence to be -Ala-Gln-Cys. These MS and MS/MS results are consistent with the peptide sequence Val-Thr-Thr-Leu-[Thr-Tyr-Gly]-Ala-Gln-Cys and with the assumption that the chromophore has a 4-(*p*-hydroxybenzylidene)imidazolinone GFP-like structure (Fig. 1).

3.2. Homology modeling and overall protein structure of phiYFP

To select a template structure for phiYFP, we aligned the amino acid sequences of GFP-like proteins with known X-ray structures. Phylogenetic analysis showed that GFP from *A. victoria* has the highest degree of homology with the phiYFP sequence (51% identity) (Fig. 2A, Supplementary Fig. S1). Likewise, phylogenetic analysis of the nearest chromophore environment of phiYFP showed the best fit (64% identity) to the 36 amino acid residues surrounding the avGFP chromophore (Fig. 2A, indicated by asterisks). Therefore, avGFP was selected as a 3D template structure (PDB code 1EMB).

Homology modeling of phiYFP was carried out with MODELLER9v7 [21]. The model is compatible with the 11-stranded β-barrel structure of avGFP (Fig. 2B), with the spatial positions of the

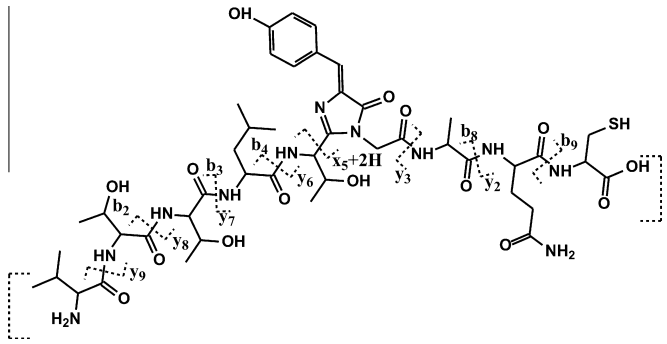

Fig. 1. MALDI-TOF/TOF MS fragmentation pattern obtained for the phiYFP pepsin-derived chromopeptide. The identified MS/MS fragments are enclosed in brackets (the *m*/*z* values and assignments of the fragments are listed in Supplementary Table S1).

important structural amino acids conserved [22]. With respect to avGFP, the calculated rms deviation of 220 aligned pairs of Cα atoms was 0.52 Å. In the middle of the central helix there is a chromophore moiety formed from the tripeptide Thr65-Tyr66-Gly67. Superposition of the phiYFP model and the avGFP crystal structure revealed a high degree of similarity within the interior of the β-barrel. There are slight deviations outside the barrel due to loop elongation between the 8-th and 9-th strands (amino acids 173-174), and in the linker region connecting the intrabarrel α-helix and the 4-th strand due to the deletion between amino acids 79 and 82 (Fig. 2B). Interestingly, loop elongation between the 8-th and 9-th strands has not been observed in other fluorescent proteins. On the other hand, deletion within the amino acid sequence 79-82 is generally characteristic of GFP-like proteins with the exceptions of avGFP [22] and aceGFP [20].

3.3. Chromophore and environment

The chromophore moiety of phiYFP is held in the correct position by multiple hydrogen bonds to the surrounding charged or polar amino acids (Fig. 3). Similarly to avGFP and to the majority of fluorescent proteins with known structures, the chromophore of phiYFP is proposed to be *cis*-coplanar. The *cis* conformation is likely to be stabilized by hydrogen bonding of the chromophore phenoxy

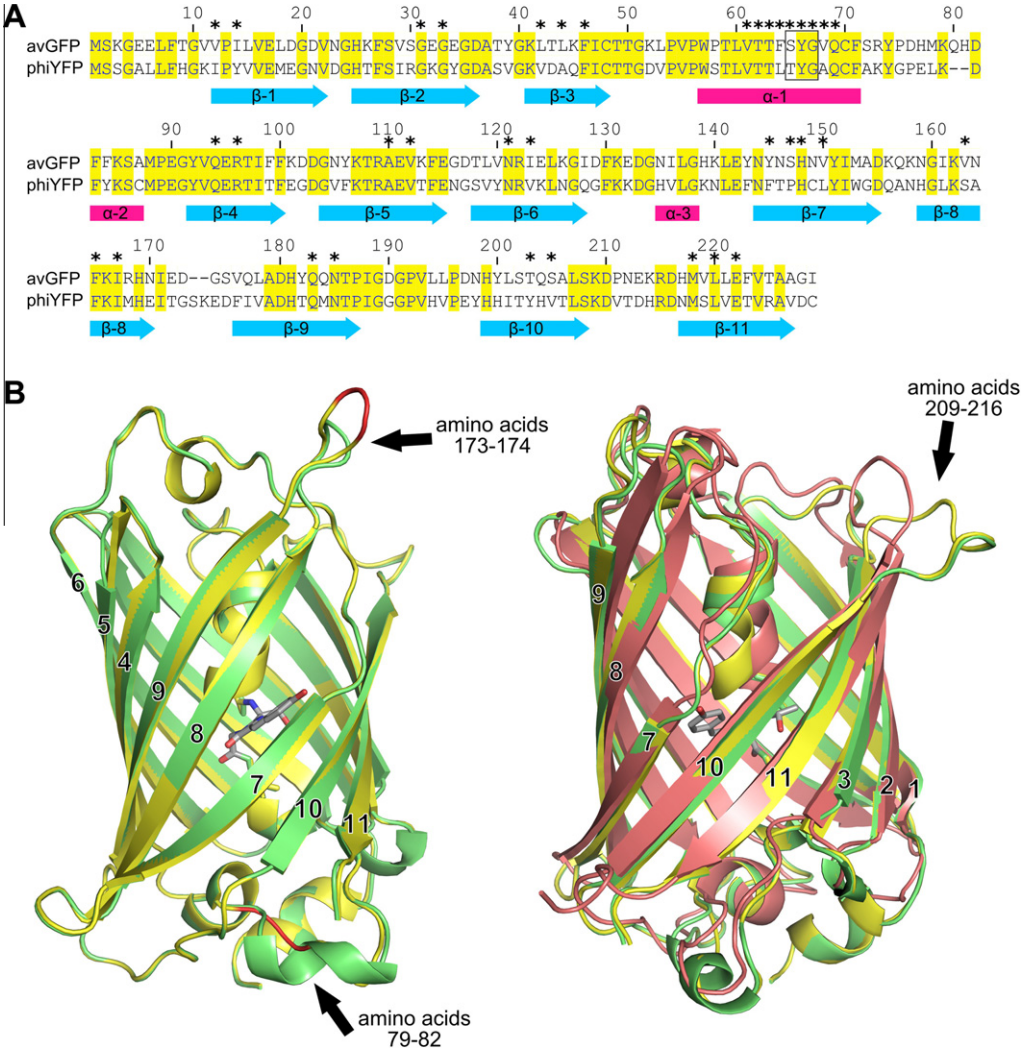

Fig. 2. Primary sequence alignment and 3D structural superposition of fluorescent proteins. (A). Sequence alignment of phiYFP and avGFP. Blue arrows and pink rectangles beneath the aligned sequences indicate β-strand and α-helix regions, respectively. Asterisks above the alignment indicate amino acids in the local chromophore environment. Identical amino acids are shaded in yellow. The chromophore-forming amino acid residues are shown in a black box. Numbering of phiYFP amino acids corresponds to the avGFP sequence. (B) Superposition of phiYFP (shown in yellow), DsRed (red) and avGFP (green) 3D structures. The phiYFP chromophore is shown in a stick representation colored gray with nitrogen and oxygen atoms colored blue and red, respectively. Differences in the structures are marked by fragments in red and by black arrows.

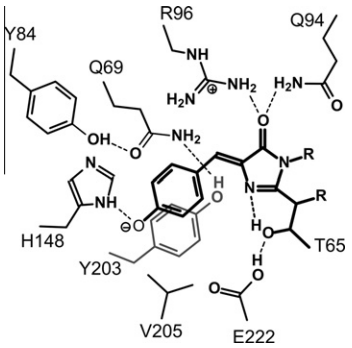

Fig. 3. Schematic representation of the immediate chromophore environment of phiYFP. The proposed positions of hydrogen bonds are shown as dashed lines. The phiYFP chromophore is shown in bold and Tyr203 in grey.

group to His148, whereas the bulky Leu150 and Phe165 residues presumably prevent *trans*-orientation of the chromophore (Fig. 3, Supplementary Fig. S2). It is clear from the model that the immediate environment of the imidazolinone ring is similar to that in avGFP. This similarity includes residues Arg96 and Glu222, which are conserved among GFP-like proteins [4,23]. Arg96 makes close contact with the imidazolinone oxygen of the chromophore, whereas Glu222 is hydrogen bonded to the imidazolinone nitrogen via the hydroxyl group of Thr65 (Fig. 3). In contrast to avGFP, Glu222 of phiYFP is not H-bonded to Ser205, which is replaced by Val. Unlike in avGFP, position 203 in phiYFP is occupied by a Tyr residue (avGFP has Thr in this position). According to our model, the aromatic ring of Tyr203 lies in the vicinity of the phenolic ring of the phiYFP chromophore providing an opportunity for π–π-stacking interactions. Mutation T203Y in avGFP was suggested to be the key factor responsible for shifting the emission peak maxima to the yellow region [17]. Another difference is the replacement of Val150 by Leu in phiYFP, which apparently prevents the chromophore *trans*-conformation and reduces the mobility of the hydroxyphenyl ring. There are also substitutions in the polypeptide sequence immediately before and after the chromophore moiety. Phe64 and Ser72 of avGFP are replaced by Leu and Ala, respectively, in phiYFP. The same mutations in YFP have been reported to facilitate protein folding [17,22,24].

3.4. Spectroscopic properties and mutational analysis

At physiological pHs, phiYFP has a strong absorption peak at 522 nm and a weak peak at 412 nm. The relative intensity of these two absorption bands is pH-sensitive with a *p*Ka value of 6.58 ± 0.02 as measured by absorbance changes at varying pH (Supplementary Fig. S3, Table 1). Like in wild-type avGFP, the two absorption peaks of phiYFP are presumably a result of a mixture of the anionic phenolate (band B) and neutral phenol (band A) forms of the chromophore. When wild-type avGFP is excited at either absorbance peak, a single fluorescence emission peak corresponding to the excited state of the anionic chromophore is detected. This phenomenon has been attributed to an excited-state proton transfer (ESPT) from the phenol hydroxyl of the chromophore to the carboxylate group of Glu222 [25–27]. In contrast, phiYFP has practically no excitation around 412 nm, while excitation at the 522 nm band produces fluorescence peak at 537 nm (Table 1). This emission peak is red-shifted by 10 nm relative to YFP (λ_{em} = 527 nm) and exhibits the longest wavelength emission maximum of all FPs that contain an unmodified *p*-HBI chromophore. Moreover, this emission maximum is very close to that of zFP538 (λ_{em} = 538 nm), which contains an extended chromophore π-electron conjugation. Similarly to YFP, the fluorescence of phiYFP is negligible when the excitation occurs at the shorter wavelength absorption band. This observation may be indicative of a predominantly radiationless internal conversion due to increased rotational freedom of the protonated chromophore. However, in contrast to YFP, both the high- and low-energy absorption bands are red-shifted as compared with those of avGFP. Based on our proposed homology model, we selected several key amino acid positions for mutagenesis and examined spectroscopic alterations resulting from these substitutions.

As indicated above, the aromatic ring of Tyr203 lies in the vicinity of the phenolic ring of the phiYFP chromophore, providing an opportunity for π–π-stacking interactions. To test the importance of these non-covalent interactions, we constructed, expressed, and purified proteins with Val and Thr substitutions at position 203. The Y203V variant exhibits major excitation and emission maxima at 512 nm and 525 nm, respectively. Because valine is aliphatic, this result implies that π–π-stacking interactions contribute only ~10 nm to the overall protein red-shift relative to avGFP (Table 1). The spectroscopic studies of the Y203V variant led us to conclude that π–π-stacking interactions are required, but alone insufficient, to explain the observed red shift of phiYFP. These results are in agreement with the spectral shifts due to π–π-stacking interactions in avGFP variants observed by Kummer et al. [28].

The Y203T mutant displays a dramatic drop in *p*Ka (Table 1) and has even further blue-shifted excitation (501 nm) and emission (516 nm) peaks. The depressed *p*Ka value of Y203T may be attributed to stabilization of the anionic state due to the formation of a

Table 1
Spectroscopic properties and *p*Ka values of phiYFP, avGFP and their variants.

Protein	Absorbance band A (nm)	Absorbance band B (nm)	Excitation (nm)	Emission (nm)	Chromophore (*p*Ka)[a]	Refs.
avGFP-wt	395	475	395/475	508/504	ND[b]	[31]
-S65T	394	489	489	511	5.95 ± 0.02	[31]
-S205V	395	~495	395/495	512/508	>11	[32]
-T203V/S205V	390	–	390	459	>11	[32]
-T203V	398	502	398/502	513/514	ND	[28]
-T203Y	404	510	404/510	524/527	ND	[28]
EGFP E222Q	387	482	482	505	5.27 ± 0.09	[19]
YFP	392	514	514	528	7.00 ± 0.03	[17]
phiYFP-wt	412	522	522	537	6.58 ± 0.02	
-Y203V	404	512	512	525	6.38 ± 0.01	
-Y203T	–[c]	500	500	516	5.2 ± 0.1	
-V205S	407	516	516	529	6.25 ± 0.03	
-T65V	410	516	516	527	7.67 ± 0.03	
-E222Q	413	517	517	530	6.62 ± 0.03	

[a] Determined by absorbance changes of bands A and B at varying pH.
[b] Not determined.
[c] Band A of the Y203T variant was not observed in the pH interval from 4.0 to 9.0.

hydrogen bond between Thr203-OH and the chromophore phenolate oxygen. A similar decrease in pKa was observed in an S65T mutant of avGFP [22]. Stabilization of the negative charge at the phenolate end of the chromophore also results in the blue-shifted spectra of Y203T. A similar blue shift has been reported for avGFP variants [29], and is consistent with a reduction in the excitation-induced shift of the negative charge towards the heterocyclic end of the chromophore [27]. This effect is missing in the Y203V variant, which means that there is decreased stabilization of the negative charge at the phenolate as compared with Y203T and approximately an extra 10 nm contribution to the phiYFP red-shift. A similar stabilization of the anionic state, albeit to a lesser extent, can occur in the V205S variant. According to the avGFP S65T crystal structure, Ser205 is H-bonded to the chromophore phenolate oxygen via an internal water molecule [22]. In phiYFP, this stabilization is evidenced by the reduced *p*Ka and the blue-shifted spectrum of the V205S variant as compared with the pKa and spectrum of the wild-type protein (Table 1).

Our homology model suggests an H-bonding pattern of Glu222 with the chromophore and surrounding amino acids that is different from the H-bonding pattern in other FPs (Fig. 3). In avGFP, the equilibrium between the anionic and neutral states of the chromophore is governed by a hydrogen bond network that brings ESPT into operation. In the case of avGFP, proton transfer occurs via a bound water molecule and the side chain oxygen of Ser205 to the carboxylate group of Glu222 [25], which is possible due to an excited-state increase in the acidity of the phenolic oxygen [30]. Importantly, in phiYFP there is no direct H-bonding network connecting Glu222 to the chromophore phenoxy group (Fig. 3). According to our model, Glu222 appears to be neutral and is H-bonded to the N2 imidazolinone nitrogen via the Thr65 hydroxyl group. The basicity of the N2 imidazolinone nitrogen of the GFP chromophore has been shown to increase significantly upon excitation. This is consistent with the *p*Ka values of 3.7 and 8.2, calculated for the ground and excited states, respectively [30]. In this model, we propose that ESPT can occur in the opposite direction from that in avGFP, which suggests an excited-state proton transfer from Glu222 to the imidazolinone nitrogen via the Thr65 side chain oxygen. Protonation of the N2 nitrogen upon excitation may explain an additional red-shift of phiYFP.

To test the role of hydrogen bonding of Thr65 to the imidazolinone nitrogen and the importance of the acidic amino acid at position 222, we constructed T65V and E222Q variants and examined spectroscopic alterations resulting from these substitutions. Replacement of Thr65 with Val leads to a blue shift in the excitation and emission maxima to 514 and 524 nm, respectively. The isosteric E222Q substitution shifts excitation to 517 nm and emission to 530 nm (Table 1). These results support the proposal that H-bonding of Glu222 to the imidazolinone nitrogen via the Thr65 hydroxyl group is an important factor in the overall red-shifted spectrum of phiYFP. The importance of H-bonding partners for the imidazolinone nitrogen has been proposed, and it has been suggested that these interactions contribute to the red-shifted spectra of the avGFP variants and EGFP [29].

In summary, a homology modeling approach in combination with mass spectrometry enabled us to propose a complete model of yellow fluorescent protein phiYFP. Based on our model, several key residues were selected for mutagenesis and the obtained variants were inspected for spectroscopic alterations. These experiments led us to conclude that multiple factors contribute to the yellow fluorescence of phiYFP. The most important structural determinants are the π–π-stacking interactions between the chromophore and Tyr203, decreased stabilization of the negative charge at the chromophore phenolate due to the absence of hydroxyl-containing aliphatic amino acids at positions 205 and 203, and hydrogen bonding of Glu222 to the imidazolinone nitrogen via the Thr65 side chain oxygen. These factors presumably operate in a cooperative manner to establish the red-shifted spectra of phiYFP.

Acknowledgments

We thank Konstantin Lukyanov, Shemyakin-Ovchinnikov Institute of Bioorganic Chemistry, Moscow, for providing the plasmid for phiYFP. This work was supported by grants from the "Molecular and Cell Biology" program of Russian Academy of Sciences, from the Russian Foundation for Basic Research (09-04-00212; 10-04-00471), from the Ministry of Science and Education in the frames of Federal special-purpose program "Scientific and science-educational personnel of innovative Russia in 2009–2013".

Appendix A. Supplementary data

Supplementary data associated with this article can be found, in the online version, at doi:10.1016/j.bbrc.2011.03.004.

References

[1] M. Zimmer, GFP: from jellyfish to the Nobel prize and beyond, Chem. Soc. Rev. 38 (2009) 2823–2832.
[2] D.M. Chudakov, M.V. Matz, S. Lukyanov, K.A. Lukyanov, Fluorescent proteins and their applications in imaging living cells and tissues, Physiol. Rev. 90 (2010) 1103–1163.
[3] A.A. Pakhomov, V.I. Martynov, GFP family: structural insights into spectral tuning, Chem. Biol. 15 (2008) 755–764.
[4] R.M. Wachter, Chromogenic cross-link formation in green fluorescent protein, Acc. Chem. Res. 40 (2007) 120–127.
[5] D.P. Barondeau, C.D. Putnam, C.J. Kassmann, J.A. Tainer, E.D. Getzoff, Mechanism and energetics of green fluorescent protein chromophore synthesis revealed by trapped intermediate structures, Proc. Natl. Acad. Sci. USA 100 (2003) 12111–12116.
[6] L.A. Gross, G.S. Baird, R.C. Hoffman, K.K. Baldridge, R.Y. Tsien, The structure of the chromophore within DsRed a red fluorescent protein from coral, Proc. Natl. Acad. Sci. USA 97 (2000) 11990–11995.
[7] A. Kikuchi, E. Fukumura, S. Karasawa, H. Mizuno, A. Miyawaki, Y. Shiro, Structural characterization of a thiazoline-containing chromophore in an orange fluorescent protein monomeric Kusabira Orange, Biochemistry 47 (2008) 11573–11580.
[8] X. Shu, N.C. Shaner, C.A. Yarbrough, R.Y. Tsien, S.J. Remington, Novel chromophores and buried charges control color in mFruits, Biochemistry 45 (2006) 9639–9647.
[9] N.V. Pletneva, S.V. Pletnev, D.M. Chudakov, T.V. Tikhonova, V.O. Popov, V.I. Martynov, A. Wlodawer, Z. Dauter, V.Z. Pletnev, Three-dimensional structure of yellow fluorescent protein zYFP538 from *Zoanthus* sp. at the resolution 1 Å, Russ. J. Bioorg. Chem. 33 (2007) 390–398.
[10] R.M. Wachter, J.L. Watkins, H. Kim, Mechanistic diversity of red fluorescence acquisition by GFP-like proteins, Biochemistry 49 (2010) 7417–7427.
[11] M.L. Quillin, D.M. Anstrom, X. Shu, S. O'Leary, K. Kallio, D.M. Chudakov, S.J. Remington, Kindling fluorescent protein from *Anemonia sulcata*: dark-state structure at 1.38 Å resolution, Biochemistry 44 (2005) 5774–5787.
[12] A.A. Pakhomov, N.V. Pletneva, T.A. Balashova, V.I. Martynov, Structure and reactivity of the chromophore of a GFP-like chromoprotein from *Condylactis gigantea*, Biochemistry 45 (2006) 7256–7264.
[13] V.I. Martynov, B.I. Maksimov, N.Y. Martynova, A.A. Pakhomov, N.G. Gurskaya, S.A. Lukyanov, A purple–blue chromoprotein from *Goniopora tenuidens* belongs to the DsRed subfamily of GFP-like proteins, J. Biol. Chem. 278 (2003) 46288–46292.
[14] A.A. Pakhomov, Y.A. Tretyakova, V.I. Martynov, Posttranslational reactions that shift spectra of asFP595 a protein from *Anemonia sulcata* towards the long-wavelength region, Russ. J. Bioorg. Chem. 36 (2010) 109–113.
[15] Y.A. Tretyakova, A.A. Pakhomov, V.I. Martynov, Chromophore structure of the kindling fluorescent protein asFP595 from *Anemonia sulcata*, J. Am. Chem. Soc. 129 (2007) 7748–7749.
[16] S.J. Remington, R.M. Wachter, D.K. Yarbrough, B. Branchaud, D.C. Anderson, K. Kallio, K.A. Lukyanov, zFP538 a yellow-fluorescent protein from *Zoanthus* contains a novel three-ring chromophore, Biochemistry 44 (2005) 202–212.
[17] R.M. Wachter, M.A. Elsliger, K. Kallio, G.T. Hanson, S.J. Remington, Structural basis of spectral shifts in the yellow-emission variants of green fluorescent protein, Structure 6 (1998) 1267–1277.
[18] D.A. Shagin, E.V. Barsova, Y.G. Yanushevich, A.F. Fradkov, K.A. Lukyanov, Y.A. Labas, T.N. Semenova, J.A. Ugalde, A. Meyers, J.M. Nunez, E.A. Widder, S.A. Lukyanov, M.V. Matz, GFP-like proteins as ubiquitous metazoan superfamily: evolution of functional features and structural complexity, Mol. Biol. Evol. 21 (2004) 841–850.

[19] J.A. Sniegowski, M.E. Phail, R.M. Wachter, Maturation efficiency trypsin sensitivity optical properties of Arg96 Glu222 and Gly67 variants of green fluorescent protein, Biochem. Biophys. Res. Commun. 332 (2005) 657–663.
[20] N.V. Pletneva, V.Z. Pletnev, K.A. Lukyanov, N.G. Gurskaya, E.A. Goryacheva, V.I. Martynov, A. Wlodawer, Z. Dauter, S. Pletnev, Structural evidence for a dehydrated intermediate in green fluorescent protein chromophore biosynthesis, J. Biol. Chem. 285 (2010) 15978–15984.
[21] A. Sali, T.L. Blundell, Comparative protein modeling by satisfaction of spatial restraints, J. Mol. Biol. 234 (1993) 779–815.
[22] M. Ormo, A.B. Cubitt, K. Kallio, L.A. Gross, R.Y. Tsien, S.J. Remington, Crystal structure of the *Aequorea victoria* green fluorescent protein, Science 273 (1996) 1392–1395.
[23] J.A. Sniegowski, J.W. Lappe, H.N. Patel, H.A. Huffman, R.M. Wachter, Base catalysis of chromophore formation in Arg96 and Glu222 variants of green fluorescent protein, J. Biol. Chem. 280 (2005) 26248–26255.
[24] T. Nagai, K. Ibata, E.S. Park, M. Kubota, K. Mikoshiba, A. Miyawaki, A variant of yellow fluorescent protein with fast and efficient maturation for cell-biological applications, Nat. Biotechnol. 20 (2002) 87–90.
[25] K. Brejc, T.K. Sixma, P.A. Kitts, S.R. Kain, R.Y. Tsien, M. Ormo, S.J. Remington, Structural basis for dual excitation and photoisomerization of the *Aequorea victoria* green fluorescent protein, Proc. Natl. Acad. Sci. USA 94 (1997) 2306–2311.
[26] G.J. Palm, A. Zdanov, G.A. Gaitanaris, R. Stauber, G.N. Pavlakis, A. Wlodawer, The structural basis for spectral variations in green fluorescent protein, Nat. Struct. Biol. 4 (1997) 361–365.
[27] M. Chattoraj, B.A. King, G.U. Bublitz, S.G. Boxer, Ultra-fast excited state dynamics in green fluorescent prote multiple states and proton transfer, Proc. Natl. Acad. Sci. USA 93 (1996) 8362–8367.
[28] A.D. Kummer, J. Wiehler, H. Rehaber, C. Kompa, B. Steipe, M.E. Michel-Beyerle, Effects of threonine 203 replacements on excited-state dynamics and fluorescence properties of the green fluorescent protein (GFP), J. Phys. Chem. B 104 (2000) 4791–4798.
[29] G. Jung, J. Wiehler, A. Zumbusch, The photophysics of green fluorescent prote influence of the key amino acids at positions 65, 203, and 222, Biophys. J. 88 (2005) 1932–1947.
[30] C. Scharnagl, R.A. Raupp-Kossmann, Solution *p*Ka values of the green fluorescent protein chromophore from hybrid quantum-classical calculations, J. Phys. Chem. 108 (2004) 477–489.
[31] M.A. Elsliger, R.M. Wachter, G.T. Hanson, K. Kallio, S.J. Remington, Structural and spectral response of green fluorescent protein variants to changes in pH, Biochemistry 38 (1999) 5296–5301.
[32] X. Shu, P. Leiderman, R. Gepshtein, N.R. Smith, K. Kallio, D. Huppert, S.J. Remington, An alternative excited-state proton transfer pathway in green fluorescent protein variant S205V, Protein Sci. 16 (2007) 2703–2710.